MATERIALS SCIENCE

Twin boundary migration mechanisms in quasi-statically compressed and plate-impacted Mg single crystals

Kelvin Y. Xie[1,2], Kavan Hazeli[1,3], Neha Dixit[1], Luoning Ma[1], K. T. Ramesh[1], Kevin J. Hemker[1]*

Twinning is a prominent deformation mode that accommodates plasticity in many materials. This study elucidates the role of deformation rate on the atomic-scale mechanisms that govern twin boundary migration. Examination of Mg single crystals deformed under quasi-static compression was compared with crystals deformed via plate impact. Evidence of two mechanisms was uncovered. Atomic-level observations using high-resolution transmission electron microscopy revealed that twin boundaries in the <*a*>-axis quasi-statically compressed single crystals are relatively smooth. At these modest stresses and rates, the twin boundaries were found to migrate predominantly via shear (i.e., disconnection nucleation and propagation). By contrast, in the plate-impacted crystals, which are subjected to higher stresses and rates, twin boundary migration was facilitated by local atomic shuffling and rearrangement, resulting in rumpled twin boundaries. This rate dependency also leads to marked variations in twin variant, size, and number density in Mg. Analogous effects are anticipated in other hexagonal closed-packed crystals.

INTRODUCTION

Deformation twinning, in addition to dislocation slip, is an important mechanism to accommodate plasticity (*1*). Unlike dislocation slip, which retains the original crystal orientation, deformation twins reorient the crystal lattice and create twin boundaries, which can substantially alter the texture and the mechanical properties of the material (*2*, *3*). In high-symmetry crystals, such as face-centered cubic (FCC) metals (in particular, the ones with low stacking fault energies), deformation twinning is prominent in materials deformed at low temperatures and high strain rates (*4*–*7*). The {111}⟨112⟩ twinning system is coplanar with the {111}⟨110⟩ slip system, and twinning can be modeled as the motion of Shockley partial dislocations on successive planes. The twin boundary migration mechanism in FCC metals is well understood: Both molecular dynamic (MD) simulations and in situ straining experiments coupled with transmission electron microscopy (TEM) suggest that Shockley partial dislocations with the (a/6)⟨112⟩ Burgers vector nucleate then glide along the {111} twin boundary to advance the twin into the matrix (*1*, *8*, *9*).

Deformation twins are also widely observed in hexagonal close-packed (HCP) metals due to the low symmetry and lack of multiple easily activated slip systems (*1*, *2*, *10*–*12*). Compared to FCC metals, deformation twinning is more profuse in deformed HCP metals (*13*–*16*). Note that the most common {10-12} twinning is not coplanar with any slip systems [(0001)⟨11-20⟩ for basal <a> slip, {10-10}⟨11-20⟩ for prismatic <a> slip, {10-11}⟨11-20⟩ for pyramidal <a> slip, {10-11}⟨11-23⟩ for pyramidal I <c + a> slip, and {11-22}⟨11-23⟩ for pyramidal II <c + a> slip]. Therefore, the deformation twinning in HCP metals is not easily derived from successive glide of partial dislocations. Moreover, the twin boundary migration mechanism has not been definitively identified; some authors prefer the shear mechanism (*17*–*20*), while others favor shuffling (*20*, *21*).

The mechanisms that govern how twin boundaries advance in HCP metals have been discussed and debated by both the computational and experimental communities. Taking the {10-12} twin as an example, some atomic simulations have suggested that the twin boundary migrates via disconnection nucleation and glide along the twin boundary, which involves predominantly shear and some shuffle (*22*–*27*). We note that many names have been used by various authors to describe these twin boundary defects, such as twinning dislocations, prismatic/basal (P/B) or basal/prismatic (B/P) interfaces, deformation faceting, and terrace defects and disconnections. In this work, we use the term "disconnections" to describe these interfacial defects on twin boundaries (*28*). For example, the lateral glide of the ⟨10-11⟩ disconnection along the {10-12} twin boundary advances the twin into the matrix by two atomic layers (*26*). When viewed as three-dimensional domains, these disconnections are "terraces," which nucleate, grow laterally, and coalesce to advance the twin boundary (*25*, *26*). Sato *et al.* (*29*) and Spearot *et al.* (*25*, *26*) also suggested that the disconnection nucleation and migration rates can be affected by a variety of parameters, such as shear stress, temperature, orientation, and structure. This predicted glide mechanism (assisted by a local shuffling) has been supported by several high-resolution TEM (HRTEM) observations of coherent twin boundaries (CTBs) decorated with disconnections (*17*–*19*). By contrast, other atomistic simulations have been interpreted to suggest that atomic shuffling alone is sufficient to advance the twin interface to achieve crystal reorientation, implying that there is no need for the shear component along the twin boundary (*20*, *21*). This atomic shuffling predominantly occurs in the two {10-12} layers of the matrix next to the twin boundary, converting basal planes to prismatic planes (and vice versa), without the action of twinning dislocations or disconnections. This pure shuffle mechanism results in highly rumpled twin boundaries and, in many cases, a loss of CTB structure in HRTEM observations (*30*–*36*). The matrix-twin misorientation angle is 86° for pure shear but falls in the range of 88° to 90° (*20*, *31*, *32*) when shuffling dominates.

[1]Department of Mechanical Engineering, Johns Hopkins University, Baltimore, MD 21218, USA. [2]Department of Materials Science and Engineering, Texas A&M University, College Station, TX 77843, USA. [3]Aerospace and Mechanical Engineering Department, The University of Arizona, Tucson, AZ 85721, USA.
*Corresponding author. Email: hemker@jhu.edu

To address this conundrum, we used Mg as the model material and characterized (using HRTEM) the atomic structures of {10-12} twin boundaries developed under two controlled and distinct deformation conditions. The {10-12} twins are of particular interest because they are easily activated (*37*), and they contribute to most plastic deformation when a Mg crystal is stretched along or compressed perpendicular to its *c* axis (*12*, *38*). To nucleate and grow {10-12} twins, we compressed Mg single crystals along the *a* axis (i.e., along a [11-20] direction) to a final 0.5% strain but at two drastically different strain rates (10^{-4} s^{-1} in quasi-static compression tests and 10^4 to 10^5 s^{-1} in plate impact tests). The detailed experimental procedure can be found in Materials and Methods. By comparing the {10-12} twin boundary characteristics in these two groups of samples, we anticipate answering the following scientific questions: (i) What is the dominant mechanism that governs twin boundary migration in quasi-statically deformed Mg? (ii) Is a new mechanism activated to drive twin boundary movement in plate-impacted Mg? In addition, (iii) if so, what leads to the switching of mechanisms?

RESULTS AND DISCUSSION

Before tackling the twin boundary migration mechanisms, it is imperative to first understand the twin structure in the postdeformed samples at mesoscale. Deformation twins are present in both quasi-statically compressed and plate-impacted samples (Fig. 1). We note that the twins in the quasi-statically compressed samples are generally thick (typically 100 to 500 μm in width), of low number density, and with only one twin variant (as an example, see Fig. 1, A to C). The low number density and thick twins can be ascribed to the low stress needed to attain 0.5% strain in quasi-statically compressed sample level (~8 MPa; see fig. S1). Under these low stresses, a small number of twins are nucleated from the most critical defects or "weakest links," and they grow to large sizes to contribute to the needed plastic strains. Only one twin variant was observed in this group of samples (labeled as T1 in Fig. 1C). Electron backscatter diffraction (EBSD) maps illustrated that T1 twins are {10-12} extension twins, and the T1 variant twins accommodate *a*-axis compression (Fig. 1C). Note that, geometrically, twins with T2 variant (also {10-12} extension twins) should have an equal chance to form (fig. S2). The experimental observation of only T1 was likely due to the slight misalignment of the crystal (~1°) in the compression tests so that nucleation and growth of T1 were favored at low stresses.

In contrast, the twins in the plate-impacted samples are relatively thin (typically 5 to 50 μm in width), of high number density, and with multiple twin variants (e.g., Fig. 1, D to F). The high number density and finer twins are due to the much higher stress levels induced by plate impact (~220 MPa; see fig. S3) combined with the very short total loading durations (~2 μs) (*39*). The higher stress level promotes additional twin nucleation from sites that would have remained inactive at lower stresses, while the short time inhibits the growth of the twin thickness. Enhanced twin nucleation leads to the higher number density and thinner twin lamellae. Three variants of primary twins (T1, T2, and T3) were observed in the plate-impacted samples (Fig. 1F). The formation of the T1 and T2 {10-12} extension twins was expected as they develop as a result of the plastic wave propagation from the impact along the <*a*>-axis. The formation of T3 twins is attributed to the uniaxial strain conditions resulting from plate impact. T3 twins are also {10-12} extension twins to the matrix, but they are not triggered by <*a*>-axis compression. During plate impact experiments, with the loading duration only ~2 μs (*39*), the expansion of the sample in a direction transverse to the impact direction is not possible because the lateral boundaries cannot be

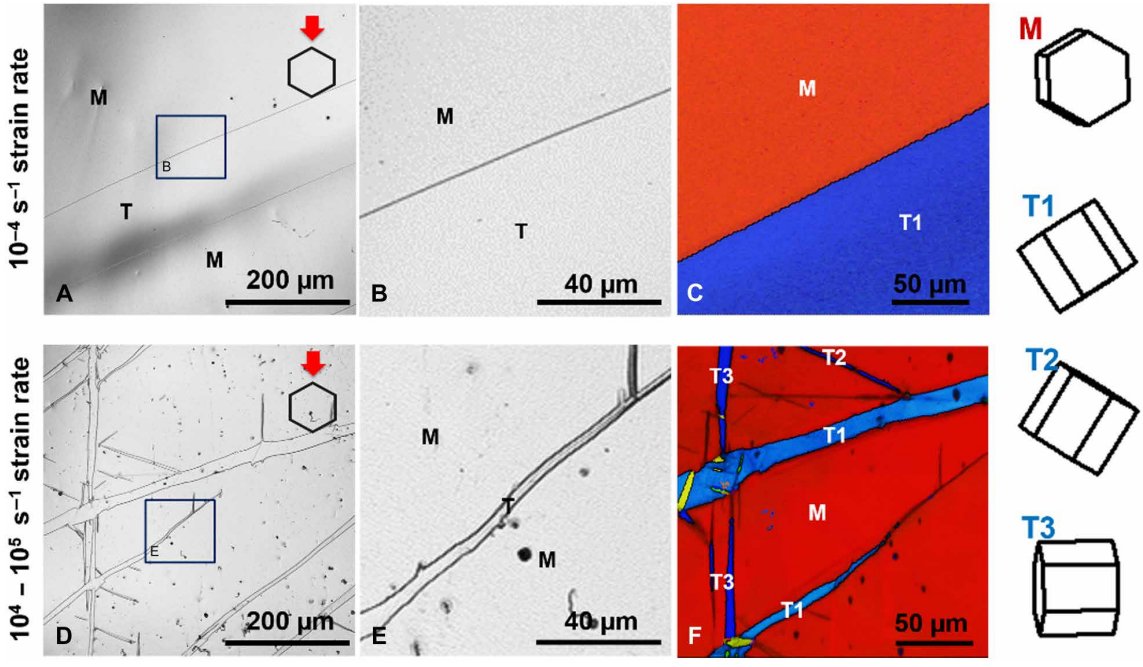

Fig. 1. Postmortem confocal micrographs and EBSD maps of <*a*>-axis Mg single crystals compressed to 0.5% plastic strain at two markedly different strain rates. The quasi-static samples had a (**A**) low number density of thick twins with (**B**) smooth twin boundaries and (**C**) only one twin variant, while the plate-impacted samples had a (**D**) high number density of fine twins with (**E**) curved twin boundaries and (**F**) three twin variants.

sensed during the experiment. In such a uniaxial strain deformation, lateral stresses are developed, which give rise to the T3 twins. Moreover, we observed that secondary twins (e.g., the yellow twin lamellae inside primary twins in Fig. 1F) were present only in the plate-impacted samples. The secondary twins were found to be {10-12} extension twins within the primary twins, and their formation can also be explained by the competition between the plastic deformation induced by plate impact and the lateral constraint with load reversal upon unloading (*39*).

The mesoscale microstructural characterization shows that {10-12} extension twins are profuse in both quasi-statically compressed and plate-impacted <*a*>-axis Mg single crystals. Although different in size, number density, and twin variant, the twins with T1 and T2 variants in both groups of samples serve the same role of accommodating the plastic deformation along the loading direction. Closer inspection of T1 and T2 twins reveals that twin boundaries in the quasi-statically compressed samples are straight (Fig. 1B), while most twin boundaries in the plate-impacted samples are curved (Fig. 1E). These apparent distinctions in the twin boundary shapes suggest that, even for the same twin variants, different mechanisms drive the twin boundary migration in response to different strain rates and loading conditions. To further test this hypothesis, we used TEM and HRTEM to provide direct atomic-level observations of the {10-12} twin boundary structures, focusing on T1 and T2 twins, and subsequently infer the attendant twin boundary migration mechanisms.

Geometrically, when the matrix and the twin are viewed along the [11-20] zone axis in TEM, the {10-12} CTB lies parallel to the electron beam and appears as a sharp interface with mirror symmetry. The nanoscale structure of twin boundaries in the quasi-statically compressed samples is consistent with this description (Fig. 2). The twin-matrix interface is composed of {10-12} CTBs decorated with disconnections (for an example, see Fig. 2A, the disconnections are indicated by white arrows). Higher-resolution micrographs of the CTBs showed that they are atomically sharp and impart mirror symmetry with an 86° misorientation between matrix and twin (Fig. 2, B and C).

The disconnections were observed to be highly mobile. Many of them were seen to glide along the CTB as a result of local heating and stresses caused by the electron beam. Artifacts associated with electron beam irradiation are generally undesirable as it changes the specimen microstructure. However, in this work, we used this artifact to provide insight into the twin boundary migration mechanisms in Mg. For example, the disconnection in Fig. 3A was originally to the right of the basal stacking fault (Fig. 3A). After slightly converging the electron beam, both the partial dislocation from the stacking fault and the disconnection on the CTB became mobile. In just 5 s, the partial dislocation ran into and terminated at the twin boundary; the disconnection glided along the twin boundary and now lay to the left of the stacking fault (their glide directions are indicated by the red arrows). The disconnection in this example is eight atomic layers in height. As the disconnection zipped along the twin boundary, it advanced the twin eight atomic layers into the matrix. Inverse fast Fourier transformation (IFFT) of the disconnection using (0002) spots from the matrix and (0-110) spots from the twin (Fig. 3C) highlighted the presence of extra half-planes at the disconnection (Fig. 3D), inferring the dislocation nature of the disconnections (detailed analysis of the disconnection can be found in fig. S4). Close inspection revealed that the disconnection contains two closely spaced edge dislocations with Burgers vectors normal to each other—one is parallel to, and the other perpendicular to, the twin boundary (fig. S4J). These dislocation-dipole–like configurations are similar to the observations made by Wang *et al.* (*27*) on the BP interfaces on the {10-12} twin boundaries in Mg. We also noticed that disconnections with different heights exhibited different mobilities. Smaller steps, such as the ones with only two atomic layers, are highly mobile, which is consistent with atomistic simulation predictions by Pond *et al.* (*40*). Many small steps were observed but escaped the field of view as soon as they were exposed to the electron beam before micrographs could be taken. Larger disconnections such as the ones in Figs. 2B and 3A are relatively less mobile and much easier to record.

Comparing the atomic-level structure of plate-impacted samples to that of quasi-statically compressed samples revealed notable differences. In the plate-impacted samples, even when the foil was tilted so that both the matrix and the twin were aligned with the [11-20] zone axis, no apparent {10-12} CTB was observed. Rather, the twin-matrix interface appears to be rumpled (Fig. 4A). Higher-magnification micrographs revealed that, although the mirror symmetry of the twin and the matrix was retained, the {10-12} twin boundaries were difficult to resolve. The contrast of the matrix-twin interface is complicated (highlighted in Fig. 4B), suggesting that the twin boundary is curved through the thickness of the TEM specimen. Moreover, the angles of misorientation between the matrices and the twins in this group of samples range from 86° to 88° (Fig. 4) instead of only 86° in the quasi-statically compressed samples. The matrix-twin interface was also imaged in thinner regions of the TEM foil, and they still lacked the well-defined {10-12} CTBs (for an example, see Fig. 4C), confirming their tortuous nature. To reveal whether there exist

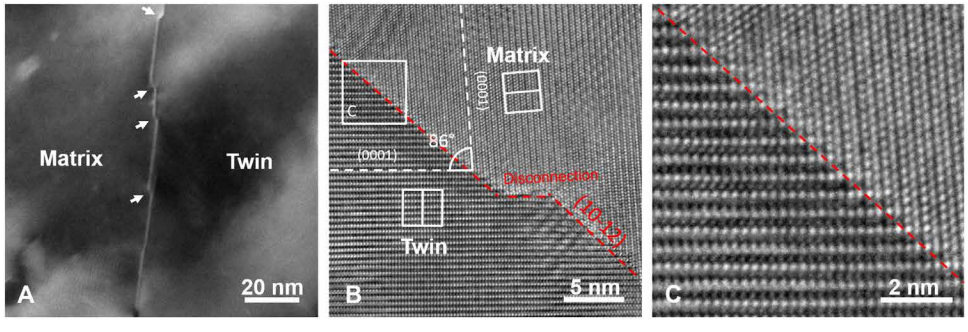

Fig. 2. The typical twin boundary structure in the quasi-statically compressed <*a*>-axis Mg single crystals. (**A**) HRTEM micrographs at a relatively low magnification showing the CTB decorated with disconnections, (**B**) closer inspection showing a disconnection, and (**C**) the {10-12} CTB. Note that the misorientation between the twin and matrix is 86°.

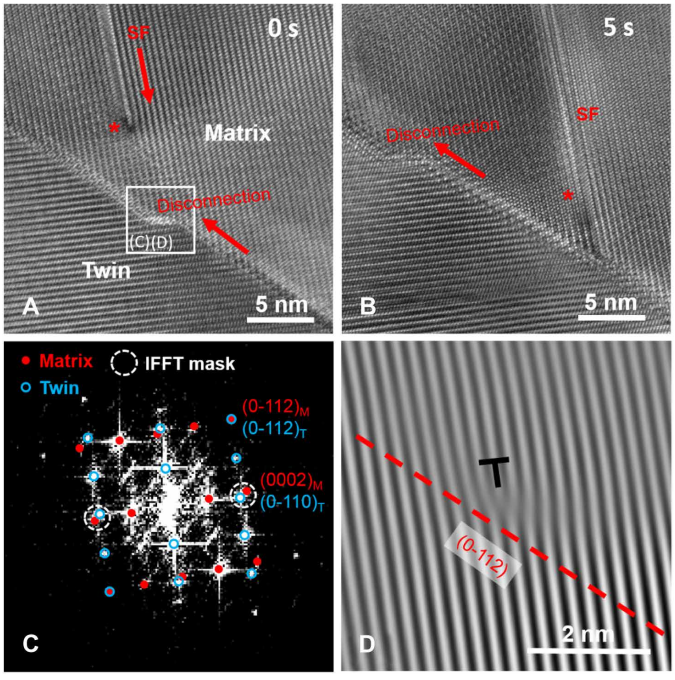

Fig. 3. Lateral glide of a disconnection on a {10-12} CTB under electron beam radiation. (**A** and **B**) HRTEM micrograph snapshots capturing the gliding of the disconnection. Note that both the disconnection and the basal Shockley partial were glissile. The disconnection glided from the right to the left of the Shockley partial/stack fault, while the basal Shockley terminated at the CTB. Note that we moved the TEM sample stage to track the disconnection, and the asterisk marks the same location in the two different micrographs. (**C**) FFT of the region containing the disconnection and (**D**) IFFT showing the dislocation nature of the disconnection.

crystallographic imperfections at the matrix-twin interface, we again performed IFFT using (0002) matrix spots and (0-110) twin spots (Fig. 4, C and D). Unexpectedly, no extra half-lattice planes were observed at the interface (Fig. 4E). It also appeared that some segments of the matrix-twin interface were {10-12} CTBs, but closer inspection revealed atomic-level unevenness (for an example, see Fig. 4F). Moreover, when slightly converging the electron beam on these twin boundaries, no apparent reconfiguration or rearrangement of the unevenness was noted, suggesting that these interfaces are more stable and less mobile than the disconnections on the CTB. Taken as a whole, these observations pointed to the fact that twin boundary migration in the plate-impacted sample was fundamentally different from how it was in the quasi-statically compressed sample.

Atomic-scale simulations have suggested that {10-12} twin boundary migration in HCP metals may be accommodated by shear (e.g., glide of disconnections) (*22*–*26*), by pure shuffling without the assistance of glissile disconnections (*20*, *21*), or both (*40*–*42*). The twin boundary migration in the quasi-statically deformed Mg is predominantly attributed to shear, where both CTBs and disconnections play very important roles (*43*). It has been proposed that disconnections nucleate on the CTB as a result of shuffling (*44*), thermal excitation (*22*), or basal <a> dislocation-CTB interactions (*19*, *23*, *45*, *46*). Once nucleated, the disconnections can glide (*40*) along the CTB in response to the external load and grow the twin at the expense of the matrix. This mechanism is similar to that of twin boundary migration in FCC crystals (*1*, *8*, *9*), albeit with larger displacements as disconnections can be much larger than partial dislocations (*22*–*24*).

In the plate-impacted samples, where disconnection formation and lateral motion may not be fast enough to accommodate the imposed strain in the very short time periods, atomic shuffling that directly advances the twin into the matrix appears to be more efficient and becomes the primary mechanism for twin boundary migration. This proposition is supported by the following observations. The twin-matrix misorientation angles (86° to 88°) deviate slightly from the theoretical value of 86°. The twin-matrix interfaces do not have CTBs and are rumpled at the atomic level. Moreover, although rumpled, twin-matrix interfaces do not contain a high density of disconnections, and the atomically rumpled features that give rise to the overall tortuous twin-matrix interface do not have glissile twin dislocations. Therefore, shear does not contribute to twin boundary migration. All these observations provide strong experimental evidence of a shuffle-dominated mechanism.

On the basis of these observations, we conclude that both shear and shuffling are active mechanisms for twin boundary migration in Mg. Which mechanism governs depends on the stress level and strain state. The shear-dominant mechanism operates when the stress level and strain rate are low, such as in the quasi-static tests (~8 MPa and 10^{-4} s^{-1} in the current work), and provides a more general mechanism to advance a twin into the matrix in HCP crystals. By contrast, the shuffling mechanism prevails when the local stress and strain rate are high (~220 MPa and 10^{4} to 10^{5} s^{-1} in the current work). In particular, in the plate impact test, the nucleation and lateral propagation of disconnections may not be fast enough to accommodate the imposed strain in a given time. Rather, most atoms at the twin boundary rearrange themselves via shuffling, resulting in the rumpled twin-matrix interface.

The competition between shear and shuffling also explains the twin boundary structure controversy in the literature. The nucleation and glide of disconnections are widely observed and prevalent in the MD simulation literature (*22*–*27*). MD simulations have also suggested that shuffling will occur and lead to a rumpled twin boundary if the disconnections fail to nucleate or are sessile once they do (*20*). Such a scenario mimics the plate-impact condition, where there is no sufficient disconnection activity to accommodate the rapid loading that accompanies the impact. In this case, shuffling is activated and directly advances the twin boundaries into the matrix. In the experimental literature, we note that the rumpled twin boundaries have historically been observed in nanopillars (*31*, *32*) and dynamically deformed HCP samples (e.g., Mg, Zr, and Co) (*30*, *33*–*36*). The high stress level in nanopillars (due to size effect) (*47*) appears to activate the shuffling mechanism and give rise to "non-CTBs" (*31*, *32*). In dynamically deformed samples involving Kolsky bar experiments, the twin boundaries are rumpled and exhibit large deviations from the twinning plane (*30*, *33*–*36*), which can be attributed to elevated stresses and strain rates and the activation of shuffling. It is worth noting that some rumpled twin boundaries have also been reported in quasi-statically deformed Mg at large strains. They were mainly found in the twin-twin interaction areas (*17*), where the local stress state is complex and the magnitude of the stress is high. It is important to point out that many twin boundary segments in the same samples remain coherent and are decorated by disconnections when they reside away from the twin-twin interactions.

Deformation twin characteristics (such as variant, size, and number density) and twin boundary migration mechanisms have been observed to be influenced by stress state, stress level, and strain rate. Mg single crystals quasi-statically compressed along the <*a*>-axis experience

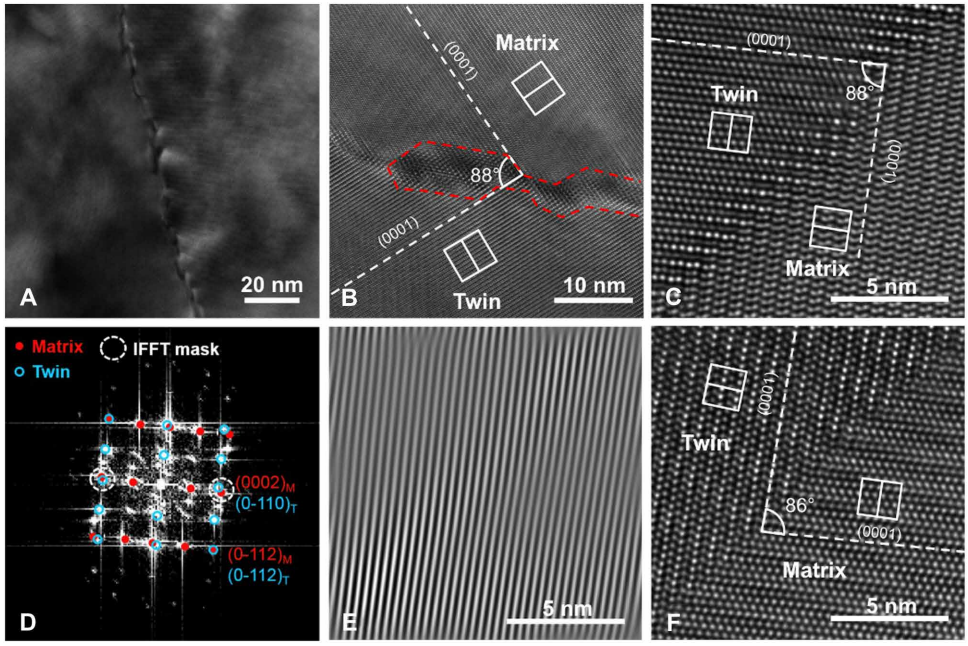

Fig. 4. The typical twin boundary structure in the plate-impacted <*a*>-axis Mg single crystals. (**A**) HRTEM micrograph revealing the typical rumpled twin boundary structure in the plate-impacted <*a*>-axis Mg single crystals. Closer inspection of (**B**) a fairly thick region and (**C**) relatively thin region showed a lack of {10-12} CTB. (**D**) FFT of (C). (**E**) The corresponding IFFT showing no dislocations present on the rumpled twin-matrix interface. (**F**) HRTEM micrograph of a twin boundary that seems to be a {10-12} CTB but not in the plate-impacted specimen. Note that the misorientation between the twin and matrix ranges from 86° to 88°.

uniaxial stress and contain low–number density thick twins and only twin variants that contribute to <*a*>-axis compression. The plate-impacted <*a*>-axis samples experienced uniaxial strain and exhibited a high number density of much thinner twins, with additional twin variants as a result of the lateral stresses associated with uniaxial strain. The mechanisms that govern twin boundary migration in these two groups of samples were found to be fundamentally different. In the quasi-statically deformed samples, flat planar twin boundaries migrated via the nucleation and glide of disconnections on CTBs, which is largely a shear process. In the plate-impacted samples, the much higher stress level and strain rate switched the twin boundary migration mechanism to local atomic rearrangement (i.e., shuffling), which resulted in rumpled and curved twin-matrix interfaces.

MATERIALS AND METHODS

Mechanical tests

Pure bulk Mg single crystals (99.999%) with [11-20] orientation were purchased from Metal Crystals and Oxides Ltd., UK. Laue diffraction confirmed that the sample was aligned to within 1° of the *a* axis of the crystals. For the quasi-static compression experiments, rectangular compression samples with dimensions of 6 mm by 6.5 mm by 14 mm were electrical discharge machined (EDM) with low power, low water pressure, and low feed rate to minimize deformation and damage. The cut surfaces were chemically polished using 10% nitric acid in water to remove the EDM recast layer. Quasi-static compression tests were conducted in an MTS machine at the strain rate of 10^{-4} s^{-1} and stopped at ~0.5% plastic strain.

For the plate impact experiments, the single-crystal target plates with 25.4 mm in diameter and 3.5 mm in thickness were electrical discharge machined using the aforementioned conditions. Both front and rear surfaces were polished gently in 15-μm B_4C lapping slurry to remove the EDM recast layer and to achieve mirror-like surfaces for interferometric measurements of the free surface velocity. The single-crystal Mg target plates were then affected by a flying plate of Mg launched by a gas gun with an impact velocity of 55 to 60 m/s. The flying plates (hot extruded pure Mg) were prepared with the same approach as the stationary single-crystal target plates. After the impact, the target was recovered using a setup designed by Jia *et al.* (*48*). The plastic strain in the impacted sample was assessed to be ~0.5% (*39*). The estimated strain rates in the plate impact experiments are in the order of 10^4 to 10^5 s^{-1}: That is eight to nine orders of magnitude higher than that in the quasi-statically compressed samples.

Microstructural characterization

Specimens for confocal microscopy, scanning electron microscopy (SEM), EBSD, and TEM were taken from the center of the deformed samples. The deformed samples were sliced using a diamond wire saw with a wire diameter of 0.125 mm, chemically polished using 5% nitric acid in water solution to remove the cutting-induced damage, and then twin-jet electropolished with 10% nitric acid in methanol at −40°C to create flat surfaces for EBSD observations and electron-transparent areas to TEM observations. All specimens were further cleaned by precision ion polishing system (PIPS) using a 0.2-keV Ar ion beam for 20 min at liquid nitrogen temperature to remove surface oxide and redeposition contamination from electropolishing. TEM specimens of nondeformed Mg single crystals prepared with this protocol showed a clean "twin-free" and "dislocation-free" microstructure, indicating that the microstructural features observed in the deformed samples are the results of quasi-static compression and plate impact, not specimen preparation. Confocal microscopy, EBSD, and TEM

observations were carried out using Keyence 3D laser scanning microscope, TESCAN MIRA3 SEM (30 kV), and Philips CM300 FEG TEM (300 kV), respectively. Since Mg is highly susceptible to electron beam damage (*49*), extra care was taken (e.g., reducing the beam current and minimizing the beam dwell time) when acquiring TEM images.

SUPPLEMENTARY MATERIALS

Supplementary material for this article is available at https://science.org/doi/10.1126/sciadv.abg3443

REFERENCES AND NOTES

1. J. W. Christian, S. Mahajan, Deformation twinning. *Prog. Mater. Sci.* **39**, 1–157 (1995).
2. I. J. Beyerlein, X. Zhang, A. Misra, Growth twins and deformation twins in metals. *Annu. Rev. Mat. Res.* **44**, 329–363 (2014).
3. S. Mahajan, D. Williams, Deformation twinning in metals and alloys. *Int. Metallurg. Rev.* **18**, 43–61 (1973).
4. F. Cao, I. J. Beyerlein, F. L. Addessio, B. H. Sencer, C. P. Trujillo, E. K. Cerreta, G. T. Gray III, Orientation dependence of shock-induced twinning and substructures in a copper bicrystal. *Acta Mater.* **58**, 549–559 (2010).
5. G. T. Gray III, High-strain-rate deformation: Mechanical behavior and deformation substructures induced. *Annu. Rev. Mat. Res.* **42**, 285–303 (2012).
6. W. Zhao, N. Tao, J. Guo, Q. Lu, K. Lu, High density nano-scale twins in Cu induced by dynamic plastic deformation. *Scr. Mater.* **53**, 745–749 (2005).
7. T. H. Blewitt, R. R. Coltman, J. K. Redman, Low-temperature deformation of copper single crystals. *J. Appl. Phys.* **28**, 651–660 (1957).
8. Y. B. Wang, M. L. Sui, E. Ma, In situ observation of twin boundary migration in copper with nanoscale twins during tensile deformation. *Philos. Mag. Lett.* **87**, 935–942 (2007).
9. N. Li, J. Wang, A. Misra, X. Zhang, J. Y. Huang, J. P. Hirth, Twinning dislocation multiplication at a coherent twin boundary. *Acta Mater.* **59**, 5989–5996 (2011).
10. M. H. Yoo, J. K. Lee, Deformation twinning in h.c.p. metals and alloys. *Philos. Mag. A* **63**, 987–1000 (1991).
11. P. G. Partridge, The crystallography and deformation modes of hexagonal close-packed metals. *Metallurg. Rev.* **12**, 169–194 (1967).
12. T. J. Balk, K. J. Hemker, L. P. Kubin, On anomalous strain hardening in iridium crystals. *Scr. Mater.* **56**, 389–392 (2007).
13. G. Proust, C. N. Tomé, G. C. Kaschner, Modeling texture, twinning and hardening evolution during deformation of hexagonal materials. *Acta Mater.* **55**, 2137–2148 (2007).
14. N. S. Prasad, N. N. Kumar, R. Narasimhan, S. Suwas, Fracture behavior of magnesium alloys – Role of tensile twinning. *Acta Mater.* **94**, 281–293 (2015).
15. M. Lentz, M. Risse, N. Schaefer, W. Reimers, I. J. Beyerlein, Strength and ductility with $\{10\bar{1}1\}$–$\{10\bar{1}2\}$ double twinning in a magnesium alloy. *Nat. Commun.* **7**, 11068 (2016).
16. J. F. Nie, Y. M. Zhu, J. Z. Liu, X. Y. Fang, Periodic segregation of solute atoms in fully coherent twin boundaries. *Science* **340**, 957–960 (2013).
17. B. M. Morrow, E. K. Cerreta, R. J. McCabe, C. N. Tomé, Toward understanding twin–twin interactions in hcp metals: Utilizing multiscale techniques to characterize deformation mechanisms in magnesium. *Mater. Sci. Eng. A* **613**, 365–371 (2014).
18. A. Serra, D. Bacon, R. Pond, Comment on "atomic shuffling dominated mechanism for deformation twinning in magnesium". *Phys. Rev. Lett.* **104**, 029603 (2010).
19. J. Zhang, G. Xi, X. Wan, C. Fang, The dislocation-twin interaction and evolution of twin boundary in AZ31 Mg alloy. *Acta Mater.* **133**, 208–216 (2017).
20. B. Li, E. Ma, Atomic shuffling dominated mechanism for deformation twinning in magnesium. *Phys. Rev. Lett.* **103**, 035503 (2009).
21. B. Li, X. Zhang, Global strain generated by shuffling-dominated twinning. *Scr. Mater.* **71**, 45–48 (2014).
22. A. Luque, M. Ghazisaeidi, W. A. Curtin, A new mechanism for twin growth in Mg alloys. *Acta Mater.* **81**, 442–456 (2014).
23. A. Serra, D. J. Bacon, A new model for {1012} twin growth in hcp metals. *Philosophical Magazine A* **73**, 333–343 (1996).
24. A. Ostapovets, P. Molnár, On the relationship between the "shuffling-dominated" and "shear-dominated" mechanisms for twinning in magnesium. *Scr. Mater.* **69**, 287–290 (2013).
25. D. E. Spearot, V. Taupin, K. Dang, L. Capolungo, Structure and kinetics of three-dimensional defects on the $\{10\bar{1}2\}$ twin boundary in magnesium: Atomistic and phase-field simulations. *Mech. Mater.* **143**, 103314 (2020).
26. D. E. Spearot, L. Capolungo, C. N. Tomé, Shear-driven motion of Mg $\{10\bar{1}2\}$ twin boundaries via disconnection terrace nucleation, growth, and coalescence. *Phys. Rev. Mater.* **3**, 053606 (2019).
27. S. Wang, M. Gong, R. J. McCabe, L. Capolungo, J. Wang, C. N. Tomé, Characteristic boundaries associated with three-dimensional twins in hexagonal metals. *Sci. Adv.* **6**, eaaz2600 (2020).
28. J. P. Hirth, J. Wang, C. Tomé, Disconnections and other defects associated with twin interfaces. *Prog. Mater. Sci.* **83**, 417–471 (2016).
29. Y. Sato, T. Swinburne, S. Ogata, D. Rodney, Anharmonic effect on the thermally activated migration of $\{10\bar{1}2\}$ twin interfaces in magnesium. *Mater. Res. Lett.* **9**, 231–238 (2021).
30. X. Y. Zhang, B. Li, X. L. Wu, Y. T. Zhu, Q. Ma, Q. Liu, P. T. Wang, M. F. Horstemeyer, Twin boundaries showing very large deviations from the twinning plane. *Scr. Mater.* **67**, 862–865 (2012).
31. B.-Y. Liu, L. Wan, J. Wang, E. Ma, Z.-W. Shan, Terrace-like morphology of the boundary created through basal-prismatic transformation in magnesium. *Scr. Mater.* **100**, 86–89 (2015).
32. B.-Y. Liu, J. Wang, B. Li, L. Lu, X.-Y. Zhang, Z.-W. Shan, J. Li, C.-L. Jia, J. Sun, E. Ma, Twinning-like lattice reorientation without a crystallographic twinning plan. *Nat. Commun.* **5**, 3297 (2014).
33. X. Y. Zhang, B. Li, Q. Liu, Non-equilibrium basal stacking faults in hexagonal close-packed metals. *Acta Mater.* **90**, 140–150 (2015).
34. J. Tu, X. Zhang, J. Wang, Q. Sun, Q. Liu, C. N. Tomé, Structural characterization of $\{10\bar{1}2\}$ twin boundaries in cobalt. *Appl. Phys. Lett.* **103**, 051903 (2013).
35. B. Xu, L. Capolungo, D. Rodney, On the importance of prismatic/basal interfaces in the growth of twins in hexagonal close packed crystals. *Scr. Mater.* **68**, 901–904 (2013).
36. D. Viladot, M. Véron, M. Gemmi, F. Peiró, J. Portillo, S. Estradé, J. Mendoza, N. Llorca-Isern, S. Nicolopoulos, Orientation and phase mapping in the transmission electron microscope using precession-assisted diffraction spot recognition: State-of-the-art results. *J. Microsc.* **252**, 23–34 (2013).
37. Q. Yu, J. Zhang, Y. Jiang, Direct observation of twinning–detwinning–retwinning on magnesium single crystal subjected to strain-controlled cyclic tension–compression in [0 0 0 1] direction. *Philos. Mag. Lett.* **91**, 757–765 (2011).
38. M. D. Nave, M. R. Barnett, Microstructures and textures of pure magnesium deformed in plane-strain compression. *Scr. Mater.* **51**, 881–885 (2004).
39. N. Dixit, L. Farbaniec, K. Ramesh, Twinning in single crystal Mg under microsecond impact along the <a> axis. *Mater. Sci. Eng. A* **693**, 22–25 (2017).
40. R. Pond, A. Serra, D. Bacon, Dislocations in interfaces in the hcp metals—II. Mechanisms of defect mobility under stress. *Acta Mater.* **47**, 1441–1453 (1999).
41. J. Wang, L. Liu, C. N. Tomé, S. X. Mao, S. K. Gong, Twinning and de-twinning via glide and climb of twinning dislocations along serrated coherent twin boundaries in hexagonal-close-packed metals. *Mater. Res. Lett.* **1**, 81–88 (2013).
42. H. El Kadiri, C. D. Barrett, M. A. Tschopp, The candidacy of shuffle and shear during compound twinning in hexagonal close-packed structures. *Acta Mater.* **61**, 7646–7659 (2013).
43. J. P. Hirth, R. C. Pond, Steps, dislocations and disconnections as interface defects relating to structure and phase transformations. *Acta Mater.* **44**, 4749–4763 (1996).
44. Q. Zu, X.-Z. Tang, S. Xu, Y.-F. Guo, Atomistic study of nucleation and migration of the basal/prismatic interfaces in Mg single crystals. *Acta Mater.* **130**, 310–318 (2017).
45. H. El Kadiri, C. D. Barrett, J. Wang, C. N. Tomé, Why are $\{10\bar{1}2\}$ twins profuse in magnesium? *Acta Mater.* **85**, 354–361 (2015).
46. A. Serra, D. Bacon, R. Pond, Dislocations in interfaces in the hcp metals—I. Defects formed by absorption of crystal dislocations. *Acta Mater.* **47**, 1425–1439 (1999).
47. M. D. Uchic, D. M. Dimiduk, J. N. Florando, W. D. Nix, Sample dimensions influence strength and crystal plasticity. *Science* **305**, 986–989 (2004).
48. D. Jia, A. Lennon, K. Ramesh, High-strain-rate pressure-shear recovery: A new experimental technique. *Int. J. Solids Struct.* **37**, 1679–1699 (2000).
49. W. Xu, Y. Zhang, G. Cheng, W. Jian, P. C. Millett, C. C. Koch, S. N. Mathaudhu, Y. Zhu, In-situ atomic-scale observation of irradiation-induced void formation. *Nat. Commun.* **4**, 2288 (2013).

Acknowledgments

Funding: This research was sponsored by the Army Research Laboratory and was accomplished under Cooperative Agreement Number W911NF-12-2-0022. The views and conclusions contained in this document are those of the authors and should not be interpreted as representing the official policies, either expressed or implied, of the Army Research Laboratory or the U.S. Government. The U.S. Government is authorized to reproduce and distribute reprints for government purposes notwithstanding any copyright notation herein. Additional support was received from the NSF under grant number DMR-1709865. **Author contributions:** K.Y.X., K.T.R., and K.J.H. designed the research. K.Y.X., K.H., and N.D. acquired data. All authors participated in data analysis and paper writing. **Competing interests:** The authors declare that they have no competing interests. **Data and materials availability:** All data needed to evaluate the conclusions in the paper are present in the paper and/or the Supplementary Materials. Additional data related to this paper are available in Craedl (https://craedl.org/project/4252055).

Submitted 28 December 2020
Accepted 25 August 2021
Published 15 October 2021
10.1126/sciadv.abg3443

Citation: K. Y. Xie, K. Hazeli, N. Dixit, L. Ma, K. T. Ramesh, K. J. Hemker, Twin boundary migration mechanisms in quasi-statically compressed and plate-impacted Mg single crystals. *Sci. Adv.* **7**, eabg3443 (2021).